HAL open science

First observation of excited states in ^{120}La and its impact on the shape evolution in the A $\approx$ 120 mass region

P.M Jodidar, C.M Petrache, B.F Lv, E.A Lawrie, A Astier, S Guo, K.K Zheng, K Auranen, A.D Briscoe, T Grahn, et al.

▶ **To cite this version:**

P.M Jodidar, C.M Petrache, B.F Lv, E.A Lawrie, A Astier, et al.. First observation of excited states in ^{120}La and its impact on the shape evolution in the A $\approx$ 120 mass region. Physics Letters B, 2024, 855, pp.138806. 10.1016/j.physletb.2024.138806 . hal-04632134

HAL Id: hal-04632134

https://hal.science/hal-04632134v1

Submitted on 11 Oct 2024

HAL is a multi-disciplinary open access archive for the deposit and dissemination of scientific research documents, whether they are published or not. The documents may come from teaching and research institutions in France or abroad, or from public or private research centers.

L'archive ouverte pluridisciplinaire **HAL**, est destinée au dépôt et à la diffusion de documents scientifiques de niveau recherche, publiés ou non, émanant des établissements d'enseignement et de recherche français ou étrangers, des laboratoires publics ou privés.

Distributed under a Creative Commons Attribution 4.0 International License

First observation of excited states in ^{120}La and its impact on the shape evolution in the $A \approx 120$ mass region

P. M. Jodidar[a], C. M. Petrache[a,], E. A. Lawrie[b], A. Astier[a], S. Guo[c,d], B. F. Lv[c,d], K. K. Zheng[c,d], K . Auranen[e], A. D. Briscoe[e,f], T. Grahn[e], P. T. Greenlees[e], A. Illana[e], H. Joukainen[e], R. Julin[e], J . Louko[e], M. Luoma[e], H. Jutila[e], J. Ojala[e], J. Pakarinen[e], A. M. Plaza[e,f], P. Rahkila[e], P. Ruotsalainen[e], J. Sarén[e], A. Tolosa-Delgado[e], J. Uusitalo[e], G. Zimba[e], I. Kuti[g], A. Krakó[g], C. Andreoiu[g], D. T. Joss[f], R. D. Page[f], E. A. Cederlöf[i], A. Ertoprak[i]

[a] *Université Paris-Saclay, CNRS/IN2P3, IJCLab, 91405 Orsay, France*
[b] *iThemba LABS, Natural Research Foundation, PO Box 722, 7129 Somerset West, South Africa*
[c] *Key Laboratory of High Precision Nuclear Spectroscopy, Institute of Modern Physics, Chinese Academy of Sciences, Lanzhou 730000, China*
[d] *School of Nuclear Science and Technology, University of Chinese Academy of Science, Beijing 100049, China*
[e] *Accelerator Laboratory, Department of Physics, University of Jyväskylä, FI-40014 Jyväskylä, Finland*
[f] *Oliver Lodge Laboratory, Department of Physics, University of Liverpool, Liverpool L69 7ZE, United Kingdom*
[g] *Institute for Nuclear Research (Atomki-ELKH), 4001 Debrecen, Hungary*
[h] *Department of Chemistry, Simon Fraser University, Burnaby, BC V5A 1S6, Canada*
[i] *KTH Department of Physics,S-10691 Stockholm, Sweden*

Abstract

Excited states have been observed for the first time in the very neutron-deficient odd-odd nucleus $^{120}_{57}\mathrm{La}_{63}$. The observed γ rays have been assigned based on coincidences with lanthanum X rays measured with the JUROGAM 3 array and with $A = 120$ fusion-evaporation residues measured with the MARA separator. The observed γ rays form a rotational band which decays to the ground state via a cascade of four low-energy transitions. Based on the systematic comparisons with the heavier odd-odd La isotopes we assign spin-parity 4^+ to the ground state and a $\pi h_{11/2} \otimes \nu h_{11/2}$ configuration to the rotational band. The nuclear shape has been investigated by the cranked Nilsson-Strutinsky model. Two quasiparticle plus triaxial rotor model calculations including the *np* interaction nicely reproduce the spin of the inversion between the even- and odd-spin cascades of $E2$ transitions, giving credit to the *np* interaction as an important parameter responsible for the mechanism inducing the inversion. The position of the Fermi levels, in particular for neutrons, also has a strong impact on the observed inversion in the chain of lanthanum nuclei.

Keywords: Nuclear reaction:^{58}Ni(^{64}Zn,pn)^{120}La; E= 255 MeV; Measured $\gamma\gamma\gamma$-coincidences; E_γ; I_γ; angular correlations; recoil gated prompt coincidences; ^{120}La deduced levels; spin and parity; model calculation.

The study of the lightest nuclei in the $A \approx 120$ mass region is confronted with the increasing difficulty of populating high-spin states using fusion-evaporation reactions due to the limited choice of projectile-target combinations and the small cross sections for neutron evaporation. The existing experimental information on excited states in very proton-rich nuclei is therefore increasingly scarce. Excited states have been identified in the extremely proton-rich odd-odd cesium nuclei up to the proton emitter ^{112}Cs [1, 2], while the odd-even Cs nuclei have been the subject of investigations devoted to the evolution of the structure and collectivity far from stability [3, 4, 5, 6, 7]. The recent studies of the odd-odd cesium nuclei have been mainly focused on chirality which was observed over a long sequence from ^{122}Cs to ^{132}Cs [8], and on signature inversion [9, 10, 11, 12, 13, 14].

The odd-odd lanthanum isotopes with $N < 82$ have also been extensively studied, with focus on chirality from ^{128}La to ^{134}La [8], and with at least two bands identified in each nucleus from ^{122}La to ^{138}La [16]. Several bands have been also observed in each of the proton-rich odd-even La nuclei, the lightest known spectroscopically being ^{121}La [16]. Two proton emitters have been discovered, ^{116}La and ^{117}La [17, 18]. However, the spectroscopic information on nuclei between the proton emitters and those known spectroscopically is missing: ^{118}La and ^{119}La are completely unknown, while ^{120}La has been synthesized but no spectroscopic information is known.

Of particular interest are the $\pi h_{11/2} \otimes \nu h_{11/2}$ bands in the odd-odd Cs and La nuclei, not only because they can have chiral partners, but also because they can exhibit the so-called *signature inversion* at low spin. The signature is defined as the symmetry in the intrinsic frame of the nucleus of the wave function which transforms as symmetric or antisymmetric with respect to 180° rotation about a principal axis. There exists a correspondence between the signature quantum number α which is 0 for even-spin and 1 for odd-spin sequences of states in the laboratory frame, but only for nuclei rotating about a principal axis of the nuclear shape. However, most often the nuclei with a collective core and active nucleons rotate or precess around an axis which is tilted relative to the principal axes of the intrinsic frame. In such cases the signature quantum number is not well defined and it is more appropriate to refer to rotational bands as built of two sequences of $E2$ transitions between states with odd and even spins, respectively, which, depending on the relative energies of the even- and odd-spin sequences can also be connected by dipole transitions. This is relevant for most odd-odd nuclei where the total angular momentum has significant components on all three nuclear axes. The $\pi h_{11/2} \otimes \nu h_{11/2}$ bands observed experimentally in the odd-odd Cs and La isotopes are composed of two branches (cascades) of $E2$ transitions, one between states with even spins and one between states with odd spins, which are connected by dipole $M1/E2$ transitions. In this work we will not use the term "signature", but will refer to the even- and odd-spin branches of the band, because our analysis suggest that the nuclear shape of ^{120}La is triaxial, and therefore the term "signature" is not applicable. Consequently, instead of the commonly used terms of "signature splitting" and "signature inversion" we will discuss the energy splitting and the inversion of the favored and unfavored branches at the crossing point.

The experimental energy splitting between the even- and odd-spin branches of a given band can be expressed as $S(I) = [E(I) - E(I-1)]/(2I)$ or $S(I) = [E(I) - E(I-1)] - [E(I+1) - E(I) + E(I-1) - E(I-2)]/2$. We will use the first simpler formula which involves the energies of only two states and can be extracted for more members of the band. One can draw two $S(I)$ curves, one for odd spins and one for even spins. When $S(I)$ of the favored branch is lower than that of the unfavored one, like for the $\pi h_{11/2} \otimes \nu h_{11/2}$ bands at high spin, there is normal splitting. When the opposite is true, there is inversion, like for the $\pi h_{11/2} \otimes \nu h_{11/2}$ bands at low spin. $S(I)$ depends on the band-head spin, which is often difficult to establish because the de-excitation of the band to low-lying states is not known. Liu *et al.* [19, 20] critically analyzed and reassigned spins of bands in the $^{118-132}$Cs and $^{124-134}$La nuclei in the 1990s, revealing the presence of low-spin inversion in all of these doubly-odd nuclei. Since then, new experimental results have been obtained for ^{116,118}Cs [9, 10, 11] and ^{122}La [21], extending further the range of nuclei which show low-spin inversion.

The inversion of the two branches observed in $A \approx 130$ and $A \approx 160$ nuclei with bands based on the $\pi h_{11/2} \otimes \nu h_{11/2}$ and $\pi h_{11/2} \otimes \nu i_{13/2}$ configurations, respectively, has been investigated theoretically using different models, aiming to unveil the mechanism at the origin of this phenomenon [22, 23, 24, 25, 26, 27, 28, 29, 30, 31, 32, 33, 34, 35, 36, 37]. Hamamoto and Matsuzaki investigated the long-range proton-neutron interaction [22, 31], Semmes and Ragnarsson [32] and Tajima [33] investigated the residual *np* contact force with a spin-spin interaction using the particle-rotor model, Hara and Sun [34] obtained the inversion within the projected shell model in $A \approx 160$ nuclei, Xu, Satula and Wyss showed that the inversion in $A \approx 130$ and $A \approx 160$ nuclei can appear in axially symmetric shapes due to the contribution of the $(\lambda\mu) = (22)$ component of the quadrupole-pairing interaction to the mean-field potential in the Total Routhian Surface (TRS)

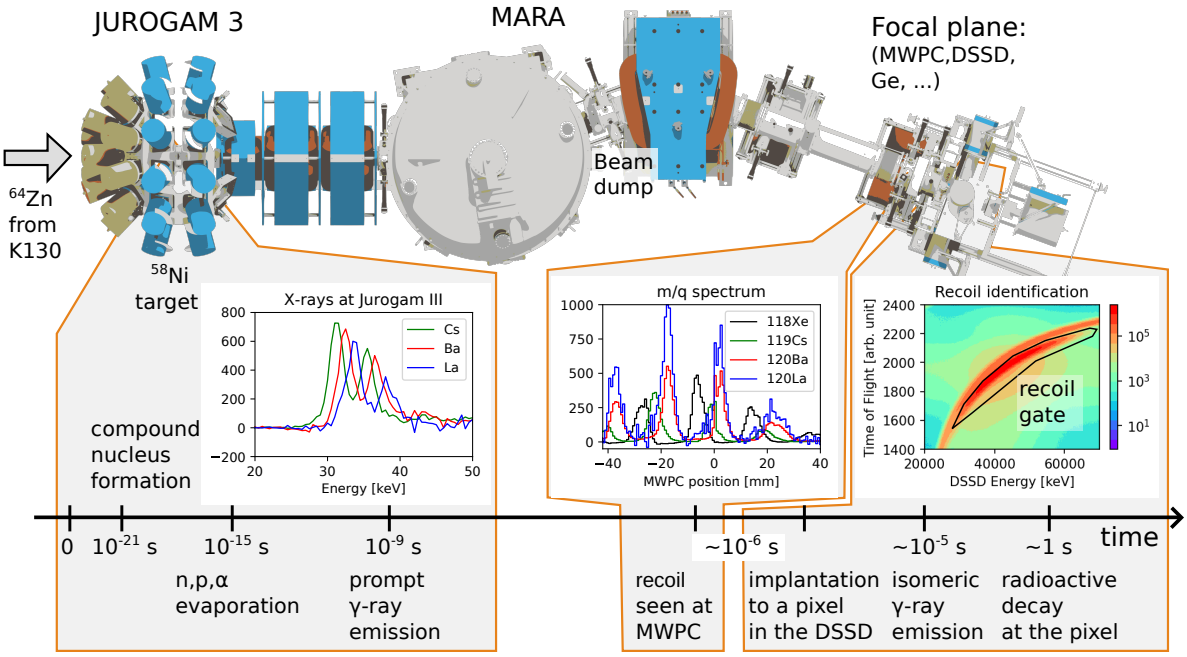

Figure 1: Schematic drawing of the MARA+JUROGAM 3 setup employed in the present experiment.

framework [35, 36]. More recently, Gao, Chen and Sun obtained excellent results in the $A \approx 130$ mass region, in particular for Cs isotopes, and interpreted the inversion phenomenon as determined by the triaxiality of the nuclear shape, while the residual interactions impact the spin of the inversion point. They also noted the manifestation of a dynamical drift of the total angular momentum toward the intermediate axis [37].

It was initially proposed [23] that inversion occurs in nuclei with triaxial shape rotating around their short axis ($\gamma > 0°$ in Lund convention), however alternative interpretations based on rotation around the intermediate axis [33, 37, 38], or around the long axis [39] were also proposed. In addition, there is no consensus on the primary quantity which governs the inversion, its amplitude, its inversion spin, and its gradual evolution along different isotopic and isotonic chains, including the La isotopes.

The most recently obtained experimental information on the lightest Cs [9, 11] and La [21, 38] nuclei, together with the present new results on ^{120}La extend the range of odd-odd nuclei exhibiting low-spin inversion, and offer the challenging opportunity to test the accuracy with which different theoretical models describe the evolution of the spin and amplitude of the inversion as a function of neutron number.

The present work reports excited states in ^{120}La. One rotational band composed of $M1/E2$ dipole and $E2$ crossover transitions was observed on top of the 8^+ state. It decays to the newly established 4^+ ground state via four low-energy dipole transitions. The spins and parities of most observed states are determined based on the systematics of the $\pi h_{11/2} \otimes \nu h_{11/2}$ bands in La nuclei and the measured angular correlation ratios. Calculations using the two quasiparticle plus triaxial rotor model including the np interaction [32, 33] reproduced very well the spin of the inversion.

The ^{120}La nucleus has been investigated using the ^{58}Ni(^{64}Zn,pn) fusion-evaporation reaction, and the JUROGAM 3 [40] plus MARA (Mass Analysing Recoil Apparatus) [41] setup at the Accelerator Laboratory of the University of Jyväskylä, Finland (see Fig. 1. A self-supporting enriched ^{58}Ni foil of 0.95 mg/cm^2 thickness was bombarded with a ^{64}Zn beam of 255 MeV delivered by the K130 cyclotron. The fusion-evaporation residues were separated as a function of A/q and identified using the in-flight double-focusing recoil mass separator MARA [42]. Three BEGe and one clover detectors surrounding the MARA focal-plane detection system were used to detect γ rays emitted by long-lived isomers and daughters of the β decay of the implanted recoils. All detector signals were recorded by the trigger-less Total Data Readout (TDR) data acquisition system, and time stamped by a global 100 MHz clock which allowed both temporal and spatial correlations to be established between recoils and events

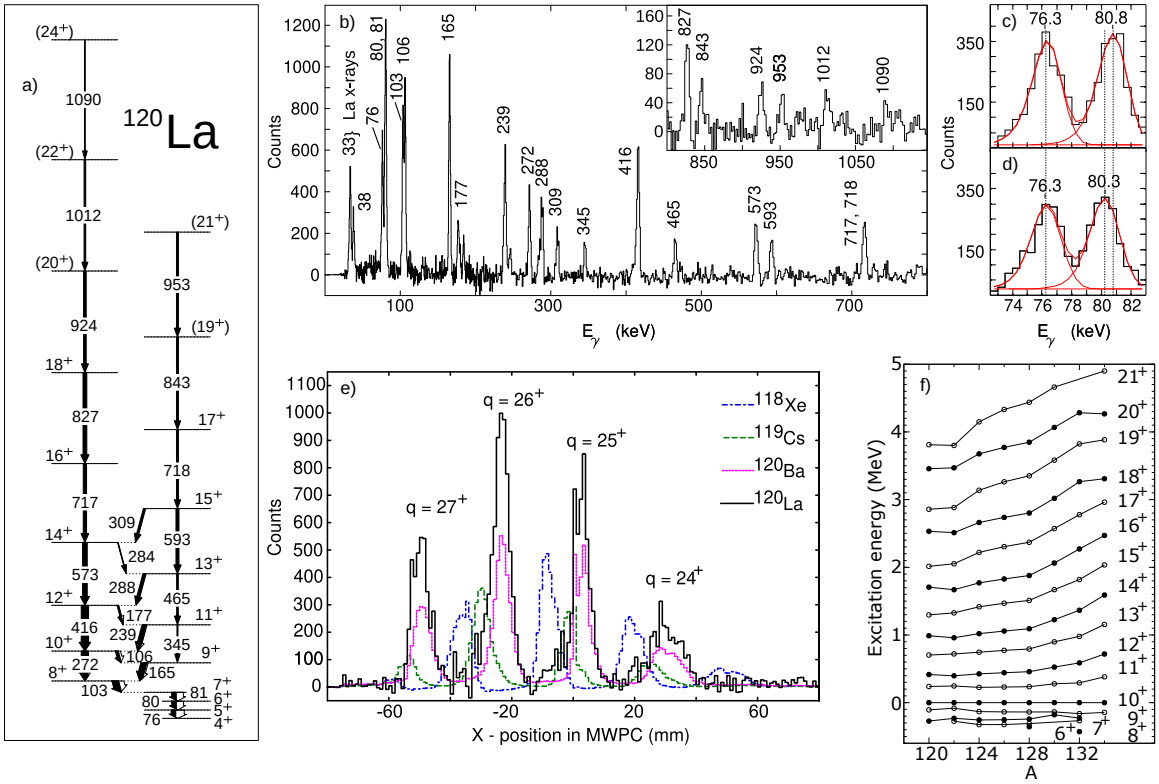

Figure 2: a) Level scheme of ^{120}La. The arrow thickness is proportional to the relative intensity of the transition. b) Spectrum showing the observed transitions in ^{120}La obtained by double-gating on the selected transitions 76-, 80-, 81-, 103-, 165-, 106-keV. c), d) Spectra showing the energy difference between the 80.3- and 80.8-keV transitions, obtained by double-gating as follow: c) on the left tail or d) on the right tail of the 81-keV peak, and on the 272-, 165-, 103-keV peaks. e) Mass spectra obtained by gating on selected transitions of ^{118}Xe, ^{119}Cs, ^{120}Ba and ^{120}La. The four peaks of ^{120}La are labeled with the charge state of the ions detected by the MWPC at the MARA focal plane. f) Excitation energy systematics of states with I $\leq 22\hbar$ relative to the 10^+ state corresponding to the $\pi h_{11/2} \otimes \nu h_{11/2}$ bands in ^{120}La (present work) and $^{122-134}$La [16].

obtained with the rest of the focal plane and JUROGAM 3 arrays [41, 43].

Prompt γ rays were detected at the target position using the JUROGAM 3 array consisting of 24 Euroball clover [44] and 15 Eurogam Phase I-type [45] escape-suppressed germanium detectors, with an efficiency of $\approx 6\%$ at 1.3 MeV. The clover detectors were arranged symmetrically relative to the direction perpendicular to the beam (twelve at 75.5° and twelve at 104.5°), while the Phase I detectors were placed at backward angles with respect to the beam direction (five at 157.6° and ten at 133.6°).

The data were sorted using the GRAIN code [46]. In a first step the newly identified bands were assigned to ^{120}La using recoil-gated prompt coincidences and the presence of x rays in the spectra. Following this identification, the analysis of the higher statistics prompt $\gamma\gamma\gamma$ coincidences without recoil gating enabled construction of the level scheme. Fully symmetrized, three-dimensional (E_γ-E_γ-E_γ) matrices were analyzed using the RADWARE [47, 48] package. A total of 3.3×10^9 prompt γ-ray coincidence events with fold ≥ 3 were collected.

The multipolarities of the γ rays were extracted using the directional correlation from oriented states ratios (R_{DCO}) and two-point angular correlation (anisotropy) ratios R_{ac} [49, 50]. The R_{DCO} values ($R_{DCO} = I_\gamma(157.6°, \approx 90°)/I_\gamma(\approx 90°, 157.6°)$) were extracted from a γ-γ matrix, constructed by sorting prompt coincidence events with the detectors at 157.6° versus those at (75.5°, 104.5°). Typical R_{DCO} values obtained by gating on a stretched quadrupole transition are $\approx$1 for stretched quadrupole and $\approx$0.46 for dipole transitions, while those obtained by gating on a stretched dipole transition are $\approx$ 1 for a dipole and $\approx$ 2.1 for a quadrupole transition. The R_{ac} values ($R_{ac} = I_\gamma(133.6°+157.6°)/I_\gamma(75.5°+104.5°)$) had typical values of 0.8 and 1.4 for stretched dipole and quadrupole transitions, respectively.

The level scheme of ^{120}La, a double-gated spectrum showing the observed transitions, and a zoom on double-gated spectra showing the evidence for the 80.3-keV and 80.8-keV transitions forming a doublet peak are given in Fig. 2. Experimental information on the γ-ray transitions is listed in Table 1.

The γ rays have been unambiguously assigned

to ^{120}La based on their prompt coincidence with the $K_{\alpha_1} + K_{\alpha_2}$ (33.4 keV) and K_{β_1} (37.8 keV) X rays of lanthanum, and on the mass spectrum measured at the MARA focal plane tagged by selected uncontaminated γ rays measured at the focus of the JUROGAM 3 array (see Fig. 2a, 2e). The mass spectrum tagged by uncontaminated γ rays assigned to ^{120}La exhibits peaks at the same positions as those of ^{120}Ba, and clearly distinct from the positions of the masses 118 and 119. In order

Table 1: Experimental information including energies E_γ, relative intensities I_γ, angular correlation R_{ac} and R_{DCO} ratios, spin-parity of the connected states of the γ rays assigned to ^{120}La. Tentative spins and parities are given in parentheses.

E (keV)	I_γ^a	R_{ac}^b	R_{DCO}	$I_f^\pi \rightarrow I_i^\pi$
76.3(5)	70(14)	0.7(1)	1.0(1)^b	$5^+ \rightarrow 4^+$
80.3(5)	70(14)	0.7(1)	1.0(1)^b	$6^+ \rightarrow 5^+$
80.8(5)	70(14)	0.7(1)	1.0(1)^b	$7^+ \rightarrow 6^+$
103.1(5)	100(15)	0.7(1)	1.1(1)^b	$8^+ \rightarrow 7^+$
106.0(5)	46(8)	0.6(1)	0.9(1)^b	$10^+ \rightarrow 9^+$
165.2(5)	89(12)	0.7(2)	0.9(1)^b	$9^+ \rightarrow 8^+$
177.2(5)	22(6)	0.6(2)		$12^+ \rightarrow 11^+$
238.7(5)	68(9)	0.9(2)		$11^+ \rightarrow 10^+$
271.5(5)	103(12)	1.4(2)	1.4(2)^b	$10^+ \rightarrow 8^+$
284(1)	10(2)			$(14^+ \rightarrow 13^+)$
288.0(5)	45(8)	0.6(1)		$13^+ \rightarrow 12^+$
308.6(5)	33(5)	1.1(1)		$15^+ \rightarrow 14^+$
345.1(5)	16(3)	1.5(3)		$11^+ \rightarrow 9^+$
415.8(5)	110(16)	1.4(2)		$12^+ \rightarrow 10^+$
465.3(5)	25(4)	1.6(3)		$13^+ \rightarrow 11^+$
573.0(5)	70(10)	1.5(3)		$14^+ \rightarrow 12^+$
593.0(5)	40(6)	1.5(3)		$15^+ \rightarrow 13^+$
717(1)	50(15)	1.5(3)		$16^+ \rightarrow 14^+$
718(1)	29(15)	1.5(3)		$17^+ \rightarrow 15^+$
827(1)	58(18)	1.3(3)		$18^+ \rightarrow 16^+$
843(1)	< 40			$(19^+ \rightarrow 17^+)$
924(1)	< 40			$(20^+ \rightarrow 18^+)$
953(1)	< 40			$(21^+ \rightarrow 19^+)$
1012(1)	< 40			$(22^+ \rightarrow 20^+)$
1090(1)	< 40			$(24^+ \rightarrow 22^+)$

^{a}Relative intensities corrected for efficiency, normalized to the intensity of the 103.1-keV transition. The intensities I_γ were obtained from a combination of those measured from the total projection and gated spectra.
^{b}Gated on the dipole 80-keV transition.

to assign the spin and parity to the ground state, which could be the long-lived $T_{1/2} = 2.8$ s isomer assigned to ^{120}La from the observation of β-delayed protons in coincidence with ^{119}Ba X rays [51], we first analyzed the systematics of the $\pi h_{11/2} \otimes \nu h_{11/2}$ bands of La isotopes. As one can see in Fig. 2f, the expected gradual evolution of the level energies can only be obtained by assigning the observed band to the $\pi h_{11/2} \otimes \nu h_{11/2}$ configuration and the band head to $I^\pi = 8^+$. The energies of the even-spin levels above 10^+ exhibit a gradual decrease with decreasing neutron number, have a minimum for ^{122}La and slightly increase for ^{120}La, while those of the odd-spin levels are nearly flat or decrease from ^{122}La to ^{120}La. This induces a significant difference between the $J^{(1)}(I)$ parameters which are related to moments of inertia (MOI) of the odd- and even-spin states in ^{120}La (see the following), being higher for the odd-spin states (see Fig. 3a, 3b).

The spin and parity of the ground state is then determined by the electromagnetic characters of the 103-, 81-, 80- and 76-keV transitions depopulating in cascade the 8^+ band head to the ground state. We established the electromagnetic characters of the four transitions by analyzing their total intensities in spectra obtained by gating on γ rays above the 8^+ state, which should be equal after correction for internal conversion. As the intensities of the four transitions are comparable (see Table 1 and Fig. 2a), but the conversion coefficients are very different for $E1$ (≈ 0.5) and $M1$ (≈ 2) characters, the four transitions should all be $E1$ or all be $M1/E2$ transitions, otherwise the intensity balance of at least one state would not be achieved. The $E1$ character is excluded by the fact that the conversion coefficient extracted from gated spectra are consistent with $M1/E2$ character, and the asymmetry in conversion coefficients expected for an $E1$ transition is not observed. Furthermore, as no enhanced low-energy electric transitions are expected in this mass region, an $E1$ character of all four transitions can be discarded. The order of the four 103-, 81-, 80- and 76-keV transitions cannot be firmly established. By gating on the 80-keV peak we find the 76-keV peak stronger than the 103-keV one after correcting for internal conversion, which suggests that the position of the 76-keV transition is below the 103-keV transition, or below the 80-keV doublet. The order of the 80- and 81-keV transitions could not be established; we tentatively put the 80-keV transition below the 81-keV one, and the 76-keV transition the lowest lying. In any case, we can then safely conclude that all four transitions of the cascade de-exciting the 8^+ state have an $M1/E2$ character leading to a spin-parity assignment of 4^+ for the ground state.

From the level energies we can extract the parameter $J^{(1)}(I) = I/\omega(I)$ related to the kinematic moment of inertia of the core and to the contributions of the valence nucleons, which are dominant at low spin. The $J^{(1)}$ parameter shown in panels a) and b) of Fig. 3 exhibits a down-sloping trend, indicating that realignments of the odd nucleons play a significant role. However, the decreasing slope becomes smaller with increasing spin and stabilises at spin around 20, beyond which the collective component

prevails.

One can distinguish three groups in the $J^{(1)}$ plots: the $J^{(1)}$ values of ^{120,122}La which are distinctly larger than those of ^{124,126,128}La especially for odd spins, and those of ^{130,132}La which are significantly lower than the others. The difference between $S(I)$ for odd and even spins shown in Fig. 3c is largest in ^{122}La at spin 12, and decreases gradually in the heavier isotopes. The spin of the inversion increases nearly linearly with increasing neutron number. The inversion persists up to the highest observed spin for ^{130}La, and for ^{132}La, ^{134}La which are not shown in Fig. 3c. Similar behavior is present in the odd-odd Cs isotopes [9].

From the transitions intensities we extracted the ratios of reduced transition probabilities $B(M1)/B(E2)$ in the rotational band of ^{120}La, which are shown together with those of the heavier La isotopes in Fig. 3d. Different to the heavier isotopes, ^{120}La exhibits a pronounced staggering over the entire observed spin range, in phase with that of the splitting $S(I)$ shown in Fig. 3c, similar to those observed in the $^{118-128}$Cs isotopes [16], but different from those of the heavier La nuclei where the regular staggering is not observed.

Before discussing the configuration assignment to the observed nuclear states we should mention that despite their common use the Nilsson quantum numbers are not very accurate for the La isotopes, as the model assumes axially symmetric nuclear shape, while the deformations of these nuclei are triaxial. On the other hand, the axial asymmetry in ^{120}La is moderate, thus in the following we will use the Nilsson labels as an indication of the dominant component in the wave function.

The spin-parity 4^+ assigned to the ground state of ^{120}La can be simply explained by coupling of a proton in the $\pi 3/2^+[422]$ Nilsson orbital to a neutron in $\nu 5/2^+[413]$, leading to the $\{\pi 3/2^+[422] \otimes \nu 5/2^+[413]\}_{4^+}$ configuration. The same reasoning can explain the spin-parity 2^+ assigned to the ground state of ^{122}La, which can be obtained by coupling a proton in the $\pi 1/2^+[420]$ orbital (which is slightly above the $\pi 3/2^+[422]$ orbital occupied in ^{120}La) to a neutron in the same $\nu 5/2^+[413]$ orbital, leading to the $\{\pi 1/2^+[420] \otimes \nu 5/2^+[413]\}_{2^+}$ configuration. The occupation of the same $\nu 5/2^+[413]$ neutron orbital in both ^{120}La and ^{122}La can be understood from the Nilsson diagram, in which the flat $\nu 5/2^+[413]$ orbital is crossed by the down-sloping $\nu 5/2^-[532]$ orbital at a deformation around $\varepsilon_2 = 0.3$: on the left side of the crossing ($\varepsilon_2 < 0.3$), the occupation of the $\nu 5/2^-[532]$ orbital corresponds to $N = 63$, that is to ^{120}La, while on the right side of the crossing ($\varepsilon_2 > 0.3$), the occupation of that orbital corresponds to $N = 65$ and ^{122}La. Concerning the $\pi h_{11/2} \otimes \nu h_{11/2}$ band in ^{120}La, the involved Nilsson orbitals are clearly $\pi 1/2^-[550]$ and $\nu 5/2^-[532]$, leading to the $\pi 1/2^-[550] \otimes \nu 5/2^-[532]$ configuration. While the ground state the spin can be calculated by summing the projections $\Omega_p + \Omega_n$ within the strong-coupling limit, such consideration is not applicable for the $\pi h_{11/2} \otimes \nu h_{11/2}$ band, because here the nucleons show considerable alignment. The band-head spin is consistent with the assumption of a nearly orthogonal coupling of the proton two single-particle angular momenta, with that of the proton nearly completely aligned with the rotation axis and that of the neutron less aligned.

In the $\pi h_{11/2} \otimes \nu h_{11/2}$ bands of the heavier La nuclei the proton occupies the same Nilsson orbital, that is $\pi 1/2^-[550]$, while the neutron successively occupies orbitals of the $h_{11/2}$ sub-shell with increasing Ω when the neutron number increases: $\nu 5/2^-[532]$ in ^{120,122}La ($N = 63, 65$), $\nu 7/2^-[523]$ in ^{124,126,128}La ($N = 67, 69, 71$), $\nu 9/2^-$ [514] in ^{130,132}La ($N = 73, 75$), and $\nu 11/2^-[505]$ in ^{134}La ($N = 77$). The occupation of these neutron orbitals is supported by the band-head spins of the single-particle bands observed in the odd-even Ba isotones of the La nuclei, which are $5/2^-$ in ^{119,121}Ba, $7/2^-$ in ^{123,125,127}Ba, $9/2^-$ in ^{129,131}Ba, and $11/2^-$ in ^{133}Ba [16].

As the occupied proton orbital remains unchanged in the chain of La nuclei, one is tempted to explain the evolution of the inversion spin with increasing neutron number through the successive occupation of the neutron Nilsson orbitals. From the $J^{(1)}$ and $S(I)$ systematics shown in Fig. 3a, 3b, 3c, we can deduce the following: the largest $J^{(1)}$ are those of ^{120,122}La in which the orbital with $\Omega = 5/2$ is occupied ($\nu 5/2^-[532]$), having therefore the angular momentum closest to the intermediate axis, which is the axis with largest moment of inertia in triaxial nuclei; the $J^{(1)}$ values of ^{124,126,128}La are clustered together and are smaller than those of ^{120,122}La because the occupied orbital has larger $\Omega = 7/2$ ($\nu 7/2^-[523]$), and therefore is more tilted relative to the intermediate axis; the $J^{(1)}$ values of ^{130,132}La are even smaller because the occupied orbital has larger $\Omega = 9/2$ ($\nu 9/2^-[514]$) and therefore more tilted relative to the intermediate axis; the $J^{(1)}$ of ^{134}La, not shown in the figure, is the smallest because the occupied $\nu 11/2^-[505]$ orbital has the largest $\Omega = 11/2$ possible in the $h_{11/2}$ sub-shell. The magnitude and variation of $J^{(1)}$ with neutron number can be directly related to the overlap of the density distribution of the occupied neutron orbital with that of the core, which depends on the orientation of the single-particle angular momentum relative to that of the nuclear axes: the orbitals with small Ω contribute more to $J^{(1)}$ because of the larger overlap with the core. For the heavy La nuclei, for which the quadrupole deformation is smaller and the triaxiality is larger, the valence neutron occupies orbitals with higher Ω values in the

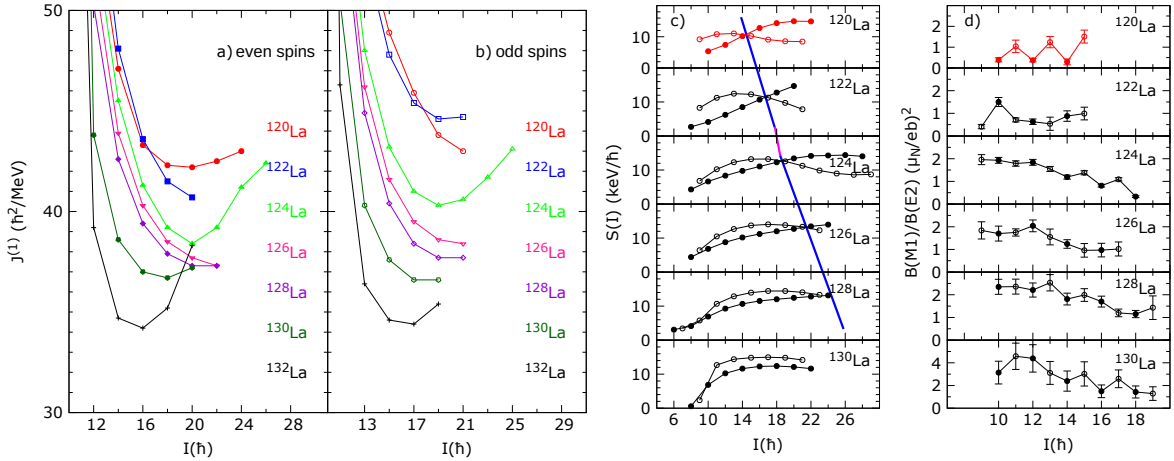

Figure 3: (Color online) a), b) Parameter $J^{(1)}$, c) splitting $S(I)$, and d) ratios of reduced transition probabilities $B(M1)/B(E2)$, for the $\pi h_{11/2} \otimes \nu h_{11/2}$ bands in ^{120}La (present work), $^{122-130}$La [21, 38, 52, 53, 54]. Filled symbols are for even spins and open symbols are for odd spins. The blue and red lines in c) are to guide the eye through the inversion points. The mixing ratio (δ) for the M1 transitions is assumed to be 0. Note that the $B(M1)/B(E2)$ values for ^{126}La have been calculated based on the intensities reported in Ref. [52], in which the $12^+ \rightarrow 10^+$ transition should be 441.7 keV instead of 411.7 keV and the $B(M1)/B(E2)$ values in panel (b) of Fig. 4 of Ref. [52] should be corrected accordingly.

$h_{11/2}$ sub-shell, inducing a strong coupling of the odd neutron with the core, and setting up favorable conditions for chiral rotation to occur.

To get a deeper insight in the mechanism responsible for the inversion, we performed two types of calculations: cranked Nilsson-Strutinsky (CNS) [55] to study the nuclear shape, and two quasiparticle plus triaxial rotor model (TQTRM) [32] to study the inversion.

The yrast rotational bands with positive parity were calculated with CNS using standard parameters for the potential [56]. The configurations near the proton Fermi level with $h_{11/2}$ nature involve 3 protons and 5 neutrons in the corresponding $h_{11/2}$ sub-shells. The potential energy surface for the yrast band and for I = 8^+ is shown in Fig. 4. The absolute minimum suggests nuclear deformation of $\varepsilon_2 = 0.29$, and γ = -19° for both branches, which is similar to that used with the core-quasiparticle coupling model for ^{124}La ($\beta_2 = 0.28$, and γ = -13°) [38]. The deduced nuclear shape indicates that rotation around the intermediate nuclear axis is favored. For $I \approx 10$ the CNS calculations predict small energy difference between the two branches of the $\pi h_{11/2} \otimes \nu h_{11/2}$ band, which increases with increasing spin. However, the experimentally observed inversion at low spins is not reproduced. Thus, additional effects, such as simultaneous rotation around more than one nuclear axis, and neutron-proton interactions, may possible play an important role in the observed inversion phenomenon. We then carried out two quasiparticle plus triaxial rotor model calculations.

We employed the two quasiparticle plus triaxial rotor model (TQTRM) of Semmes and Ragnarsson [32] with standard parameters for the Nilsson potential [56] and for the pairing gaps, resulting in $\Delta_p = 1.242$ MeV and $\Delta_n = 1.113$ MeV. The Fermi level for protons is lying near the lowest-energy $h_{11/2}$ orbital (dominant $\Omega_\ell = 1/2$) and for neutrons between the second and third $h_{11/2}$ orbitals (dominant $\Omega_\ell = 3/2, 5/2$). Calculations included large configuration spaces comprising four (five) negative-parity orbitals near the proton (neutron) Fermi level. The orbitals have mostly $h_{11/2}$ nature. The Fermi level for protons is lying near the lowest-energy $h_{11/2}$ orbital (dominant $\Omega_\ell = 1/2$) and for neutrons between the second and third $h_{11/2}$ orbitals (dominant $\Omega_\ell = 3/2, 5/2$).

The TQTRM moments of inertia follow the irrotational flow model dependence with respect to γ, an assumption that is supported by empirical evaluations [57]. The choice of the magnitude of the moment of inertia was guided by the energy of the 2^+ state of the even-even core and no variable MOI was used. A Coriolis attenuation factor of 0.7 was adopted, as in previous works in this mass region [33]. The model includes residual neutron-proton interaction in the form

$$V_{np} = \sqrt{8\pi^3}\left(\frac{\hbar}{m\omega}\right)^{\frac{3}{2}} \delta(r_p - r_n)(u_0 + u_1 \sigma_p \cdot \sigma_n),$$

with parameters $u_0 = -7.2$ MeV and $u_1 = -0.8$ MeV, which were previously established for the $\pi h_{11/2} \otimes \nu h_{11/2}$ configuration [12, 32].

Results from the TQTRM calculations carried out with quadrupole deformation of $\varepsilon_2 = 0.28$ and $\gamma = 16°$ are shown in Fig. 4, where one can see that both the calculated excitation energies and the inversion spin were very well reproduced.

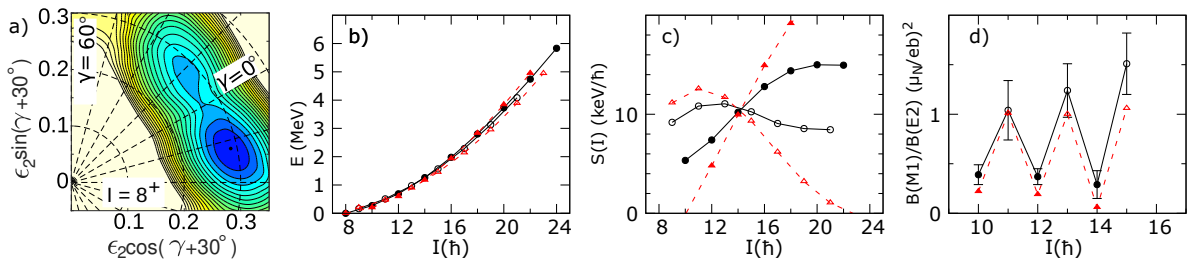

Figure 4: (Color online) a) CNS potential energy surface plot for the 8^+ state of the $\pi h_{11/2} \otimes \nu h_{11/2}$ band in ^{120}La. The contour lines are 250 keV apart. b) excitation energies, c) splitting $S(I)$ and d) $B(M1)/B(E2)$ ratios calculated with TQTRM (red triangles) and experimental (black circles) for the $\pi h_{11/2} \otimes \nu h_{11/2}$ band in ^{120}La. The lines are drawn to guide the eyes. Open symbols are for odd spins and filled symbols for even spins.

It is known that the inversion is a result of multiple effects, such as the position of the Fermi levels (in particular if they are close to an Ω=1/2 orbital), triaxiality of the nuclear shape, and residual neutron-proton interactions. For ^{120}La the present calculations suggest that most important for the observed inversion is the position of the Fermi levels, in particular the neutron Fermi level. Significant inverse splitting was found specifically for wave-function contributions where the second lowest-energy $\nu h_{11/2}$ orbital was involved.

Transition probabilities were calculated using effective spin and core g factors of $g_{s,eff} = 0.8\ g_{s,free}$ and $g_c = Z/A$, respectively. The model calculates macroscopically the electric quadrupole moment assuming that the nucleus is a deformed rigid object with a sharp surface. It is known that this assumption is a simplification. In the present calculations it resulted in an overestimation of the reduced $B(E2)$ values for the intra-band transitions, for instance a theoretical value of $B(E2; 10^+ \rightarrow 8^+) = 216$ W.u. was obtained in the calculations, while typical values of $\sim$ 100 W.u. are expected, similar to the measured $B(E2; 2^+ \rightarrow 0^+) = 113(5)$, 94(4) W.u. in the neighboring ^{124,126}Ba, and $B(E2; 2^+ \rightarrow 0^+) = 138(24)$ W.u. in ^{126}Ce, [16]. Thus, to reduce the theoretical electric quadrupole moment we used an effective electric charge $e_{eff} = 0.8e$, which resulted in a reasonable $B(E2; 10^+ \rightarrow 8^+) = 97$ W. u.

There is a very good agreement between the calculated $B(M1)/B(E2)$ ratios and the experimental observations. In particular the staggering, which is clearly see at low spin only in ^{120}La, is very well reproduced, both in its phase and magnitude, see Fig. 4c. It is caused by a staggering in the $B(M1)$ values, which are very sensitive to the triaxial deformation. It is interesting to note that the calculated $B(M1)$ staggering decreases for larger triaxiality, which could explain the experimentally observed lack of staggering for the heavier La isotopes, where larger triaxial deformation is expected.

Summarizing, the present work reports for the first time spectroscopic data in ^{120}La, the lightest La isotope in which a collective rotational band built on the $\pi h_{11/2} \otimes \nu h_{11/2}$ configuration has been observed. The band properties are theoretically investigated with the cranked Nilsson-Strutinsky model, and the two quasiparticle plus triaxial rotor model including the np interaction. An excellent agreement is obtained for the spin where the inversion between the $E2$ cascades of the $\pi h_{11/2} \otimes \nu h_{11/2}$ band occurs, giving credit to the np interaction as an important parameter responsible for the inversion. The calculations also suggest that the position of the Fermi levels, in particular for neutrons, have a strong impact on the observed inversion. Significant inverted splitting was found when the second lowest-energy neutron orbital from the $h_{11/2}$ subshell was involved.

The work is based on research supported in part by the National Research Foundation of South Africa (Grant Number 150650); by the National Natural Science Foundation of China (Grants No. 12305128), by the Hubert Curien Partnership (PHC) "Cai Yuanpei Project", by the International Partnership Program of Chinese Academy of Sciences for Future Network (Grants No. 016GJHZ2023024FN); by the Academy of Finland under the Finnish Centre of Excellence Programme (2012-2017); by the EU 7th Framework Programme Project No. 262010 (ENSAR); by the United Kingdom Science and Technology Facilities Council through grant numbers ST/P004598/1 and ST/V001027/1, by the National Research, Development and Innovation Fund of Hungary (Project No. K128947), as well as by the European Regional Development Fund (Contract No. GINOP-2.3.3-15-2016-00034); by the Polish National Science Centre (NCN) Grant No. 2013/10/M/ST2/00427; by the Swedish Research Council under Grant No. 2019-04880; and by the National Natural Science Foundation of China (Grants No. 11505242, No. 11305220, No. U1732139, No. 11775274, and No. 11575255). The use of germanium detectors from the GAMMAPOOL is acknowledged. I.K. was supported by National Research, Development and Innovation Office-NKFIH, contract number PD 124717.

[1] P. T. Wady *et al.*, Phys. Rev. C 85 (2012)

034329. doi:10.1103/PhysRevC.85.034329.

[2] J. F. Smith *et al.*, Phys. Rev. C 73 (2006) 061303. doi:10.1103/PhysRevC.73.061303.

[3] P. T. Wady *et al.*, Phys. Lett. B 740 (2015) 243. doi:10.1016/j.physletb.2014.11.045.

[4] J. F. Smith *et al.*, Phys. Rev. C 63 (2006) 024319. doi:10.1103/PhysRevC.63.024319.

[5] K. K. Zheng *et al.*, Phys. Rev. C 104 (2021) 044305. doi:10.1103/PhysRevC.104.034305, [link].
URL https://doi.org/10.1103/PhysRevC.104.044305

[6] C. B. Moon, T. Komatsubara, K. Furuno, Journal Korean Physical Society 38 (2001) 83.

[7] A. Gizon *et al.*, Eur. Phys. J. A 8 (2012) 41. doi:0.1007/s10050-000-4503-0.

[8] B. Xiong, Y. Wang, Nuclear chiral doublet bands data tables, Atomic Data and Nuclear Data Tables 125 (2019) 193 – 225. doi:https://doi.org/10.1016/j.adt.2018.05.002.
URL http://www.sciencedirect.com/science/article/pii/S0092640X18300329

[9] J. F. Smith *et al.*, Phys. Rev. C 74 (2006) 034310. doi:10.1103/PhysRevC.74.034310.

[10] J. F. Smith *et al.*, Phys. Lett. B 406 (1997) 7. doi:10.1016/S0370-2693(97)00651-5.

[11] K. K. Zheng *et al.*, Phys. Rev. C 104 (2021) 044325. doi:10.1103/PhysRevC.104.034325, [link].
URL https://doi.org/10.1103/PhysRevC.104.044325

[12] B. Cederwall *et al.*, Nucl. Phys. A 542 (1992) 454. doi:https://10.1016/0375-9474(92)90106-T, [link].
URL https://doi.org/10.1016/0375-9474(92)90106-T

[13] C.-B. Moon *et al.*, Nucl. Phys. A 696 (2001) 45. doi:10.1016/S0375-9474(01)01118-6, [link].
URL https://doi.org/10.1016/S0375-9474(01)01118-6

[14] J. F. Smith *et al.*, Phys. Rev. C 58 (1998) 3237. doi:10.1103/PhysRevC.58.3237.

[15] C. Thibault *et al.*, Hyperfine structre and isotope shift of the d2 line of 118-145cs and some of their isomers, Nucl. Phys. A 367 (1981) 1. doi:10.1016/0375-9474(81)90274-8.
URL https://doi.org/10.1016/0375-9474(81)90274-8

[16] NNDC Online Data Service, ENSDF database, http://www.nndc.bnl.gov/ensdf/.

[17] W. Zhang *et al.*, Nature Communication Physics 5 (2022) 285. doi:10.1038/s42005-022-01069-w.

[18] Z. Liu *et al.*, Phys. Lett. B 702 (2011) 24. doi:10.1016/j.physletb.2011.06.058.

[19] Y. Liu *et al.*, Phys. Rev. C 54 (1996) 719. doi:10.1103/PhysRevC.54.719.

[20] Y. Liu *et al.*, Phys. Rev. C 58 (1998) 1849. doi:10.1103/PhysRevC.58.1849.

[21] M. Fantuzi *et al.*, Nuclear spectroscopy near the proton drip line in the lanthanide region: The122la nucleus, Eur. Phys. J. A 38 (1) (2008) 43–51. doi:10.1140/epja/i2008-10650-2.
URL https://doi.org/10.1140/epja/i2008-10650-2

[22] I. Hamamoto, B. Mottelson, Phys. Lett. B 167 (1986) 370. doi:10.1016/0370-2693(86)90486-7.

[23] R. Bengtsson, H. Frisk, F. R. May, J. A. Pinston, Nucl. Phys. A 54415 (1984) 189. doi:10.1016/0375-9474(84)90620-1.

[24] S. Frauendorf, F. R. May, Phys. Lett. B 125 (1983) 245. doi:10.1016/S0375-9474(97)00004-3.

[25] I. Hamamoto, B. Mottelson, Phys. Lett. B 127 (1983) 281. doi:10.1016/0370-2693(83)91000-6.

[26] I. Hamamoto, B. Mottelson, Phys. Lett. B 132 (1983) 7. doi:10.1016/0370-2693(86)90486-7.

[27] A. Ikeda, S. Åberg, Nucl. Phys. A 480 (1988) 85. doi:10.1016/0375-9474(88)90386-7.

[28] M. Matsuzaki, Nucl. Phys. A 504 (1989) 456. doi:10.1016/0375-9474(89)90552-6.

[29] B. Cederwall *et al.*, Nucl. Phys. A 542 (1992) 454. doi:10.1016/0375-9474(92)90106-T.

[30] I. Hamamoto, Phys. Lett. B 179 (1986) 327. doi:10.1016/0370-2693(86)90486-7.

[31] M. Matsuzaki, Phys. Lett. B 269 (1991) 23. doi:10.1016/0370-2693(91)91445-2.

[32] P. B. Semmes, I. Ragnarsson, Proc. of Int. Conf. on High-Spin Phys. and Gamma-Soft Nuclei, Pittsburgh, 1990 World Scientific, Singapore, 1991. p. 500.

[33] N. Tajima, Nucl. Phys. A 572 (1994) 365. doi:10.1016/0375-9474(94)90180-5.

[34] K. Hara, Y. Sun, Nucl. Phys. A 531 (1991) 221. doi:10.1016/0375-9474(91)90610-I.

[35] W. Satula, R. Wyss, Acta Phys. Pol. B 27 (1996) 121.

[36] F. R. Xu, W. Satula, R. Wyss, Nucl. Phys. A 669 (2000) 119. doi:S0375-9474?99.00817-9.

[37] Z. C. Gao, Y. S. Chen, Y. Sun, Phys. Lett. B 634 (2006) 195. doi:10.1016/j.physletb.2006.01.033.

[38] H. J. Chantler *et al.*, Signature inversion in doubly odd ^{124}La, Phys. Rev. C 66 (2002) 014311. doi:10.1103/PhysRevC.66.014311.
URL https://link.aps.org/doi/10.1103/PhysRevC.66.014311

[39] E. Gueorguieva *et al.*, Phys. Rev. C 69 (2004) 044320. doi:10.1103/PhysRevC.69.044320.

[40] J. Pakarinen *et al.*, Eur. Phys. J. A 56 (2020) 149. doi:10.1140/epja/s10050-020-00144-6.

[41] J. J. Uusitalo, J. Sarén, J. Partanen, J. Hilton, Acta Phys. Pol. B 50 (2019) 319. doi:10.5506/APhysPolB.50.319.

[42] J. Sarén *et al.*, Nucl. Instr. Meth. Phys. Res. A 266 (2008) 4196. doi:10.1016/j.nimb.2008.05.027, [link].
URL https://doi.org/10.1016/j.nimb.2008.05.027

[43] J. Hilton *et al.*, Phys. Rev. C 100 (2019) 014305. doi:10.1103/PhysRevC.100.014305.

[44] G. Duchêne *et al.*, Nucl. Instr. Meth. Phys. Res. A 432 (1999) 90. doi:10.1016/S0168-9002(99)00277-6, [link].
URL https://doi.org/10.1016/S0168-9002(99)00277-6

[45] C. W. Beausang *et al.*, Nucl. Instr. Meth. Phys. Res. A 313 (1992) 37. doi:10.1016/0168-9002(92)90084-H, [link].
URL https://doi.org/10.1016/0168-9002(92)90084-H

[46] P. Rahkila, Graina java data analysis system for total data readout, Nucl. Instrum. Meth. Phys. Res. A 595 (1) (2008) 637–642. doi:doi:10.1016/j.nima.2008.08.039.
URL https://doi.org/10.1016/j.nima.2008.08.039

[47] D. Radford, {ESCL8R} and levit8r: Software for interactive graphical analysis of {HPGe} coincidence data sets, Nucl. Instrum. Meth. Phys. Res. A 361 (1–2) (1995) 297 – 305. doi:http://dx.doi.org/10.1016/0168-9002(95)00183-2.
URL http://www.sciencedirect.com/science/article/pii/0168900295001832

[48] D. Radford, Background subtraction from in-beam {HPGe} coincidence data sets, Nucl. Instrum. Meth. Phys. Res. A 361 (1–2) (1995) 306 – 316. doi:http://dx.doi.org/10.1016/0168-9002(95)00184-0.
URL http://www.sciencedirect.com/science/article/pii/0168900295001840

[49] A. Krämer-Flecken, T. Morek, R. M. Lieder, W. Gast, G. Hebbinghaus, H. M. Jäger, W. Urban, Use of dco ratios for spin determination in γ-γ coincidence measurements, Nucl. Instrum. Meth. Phys. Res. A 275 (2) (1989) 333 – 339. doi:10.1016/0168-9002(89)90706-7.
URL http://www.sciencedirect.com/science/article/pii/0168900289907067

[50] C. J. Chiara *et al.*, Probing *sd-fp* cross-shell interactions via terminating configurations in ^{42,43}Sc, Phys. Rev. C 75 (2007) 054305. doi:10.1103/PhysRevC.75.054305.
URL http://link.aps.org/doi/10.1103/PhysRevC.75.054305

[51] J. Nitschke, P. Wilmarth, P. Lemmertz, W.-D. Zeitz, J. Honkanen, Zeit. Phys. A 316 (1984) 249. doi:10.1007/BF01412274.

[52] K. Y. Ma, J. B. Lu, S. P. Ruan, D. Yang, J. Li, Y. Z. Liu, Y. J. Ma, X. G. Wu, Y. Zheng, C. Y. He, Observation of a second $\pi h_{11/2} \bigotimes \nu h_{11/2}$ band in ^{126}la, Phys. Rev. C 88 (2013) 057302. doi:10.1103/PhysRevC.88.057302.
URL https://link.aps.org/doi/10.1103/PhysRevC.88.057302

[53] K. Y. Ma, J. B. Lu, D. Yang, H. D. Wang, Y. Z. Liu, X. G. Wu, Y. Zheng, C. Y. He, Spin assignments of rotational bands in ^{128}la, Phys. Rev. C 86 (2012) 027301. doi:10.1103/PhysRevC.86.027301.
URL https://link.aps.org/doi/10.1103/PhysRevC.86.027301

[54] M. Ionescu-Bujor *et al.*, Lifetime measurements in the chiral-candidate doublet bands of ^{130}La, Phys. Rev. C 98 (2018) 054305. doi:10.1103/PhysRevC.98.054305.
URL https://link.aps.org/doi/10.1103/PhysRevC.98.054305

[55] B. G. Carlsson, I. Ragnarsson, Calculating the nuclear mass in the very high angular momentum regime, Phys. Rev. C 74 (2006) 011302. doi:10.1103/PhysRevC.74.011302.
URL https://link.aps.org/doi/10.1103/PhysRevC.74.011302

[56] T. Bengtsson, I. Ragnarsson, Nucl. Phys. A 436 (1985) 14. doi:10.1016/0375-9474(85)90541-X.

[57] J. Allmond, J. Wood, Empirical moments of inertia of axially asymmetric nuclei, Physics Letters B 767 (2017) 226–231. doi:https://doi.org/10.1016/j.physletb.2017.01.072. URL https://www.sciencedirect.com/science/article/pii/S0370269317300916